Manuscript Details

Manuscript number	JAAP_2018_932
Title	Degradation of wood by UV light: a study by EGA-MS and Py-GC/MS with on line irradiation system
Article type	Research Paper

Abstract

UV degradation of wood is an important phenomenon that entails loss of aesthetic and mechanic properties. The changes are usually studied with artificial ageing followed by spectroscopy, and focus on colour changes. Analytical pyrolysis coupled with gas chromatography-mass spectrometry (Py-GC/MS) and evolved gas analysis-mass spectrometry (EGA-MS) are powerful tools for wood characterisation, but the change in pyrolytic behaviour of wood after UV irradiation is not well documented. In this work, a new instrumental setup was used to perform UV irradiation on line with EGA-MS and Py-GC/MS with in situ derivatisation of fir and chestnut wood. The effect of UV exposure was evaluated in terms of thermal stability and composition of the pyrolysate. The results showed that UV degradation of wood is strongly related to its lignin content. Fir wood, with higher lignin content, showed extensive degradation after 4 hours of irradiation, while chestnut wood, with lower lignin content, showed very small changes. Holocellulose to lignin ratios (H/L) were calculated, and principal component analysis was performed on the results of Py-GC/MS, revealing that this technique could be used as a fast monitoring tool to assess the UV degradation of wood.

Keywords	analytical pyrolysis; evolved gas analysis; UV degradation; biomass; wood; lignin
Manuscript category	Analytical - archaeometry, cultural heritage, environmental, biomass, food

Corresponding Author	Marco Mattonai
Corresponding Author's Institution	Department of Chemistry and Industrial Chemistry, University of Pisa
Order of Authors	Marco Mattonai, Atsushi Watanabe, Ai Shiono, Erika Ribechini
Suggested reviewers	Cristian Torri, Dietrich Meier, Kaige Wang, Taina Ohra-aho

Submission Files Included in this PDF

File Name [File Type]

CoverLetter.doc [Cover Letter]

Manuscript.docx [Manuscript File]

Figure 1.tif [Figure]

Figure 2.tif [Figure]

Figure 3.tif [Figure]

Figure 4.tif [Figure]

To view all the submission files, including those not included in the PDF, click on the manuscript title on your EVISE Homepage, then click 'Download zip file'.

UNIVERSITÀ DI PISA

Marco Mattonai
Tel. +39 0502219312
E-mail: mmattonai@gmail.com
http://www.dcci.unipi.it

DIPARTIMENTO DI CHIMICA E CHIMICA INDUSTRIALE

Via Giuseppe Moruzzi, 13
56124 Pisa (Italy)
Cod. Fisc. 80003670504
P. IVA 0028682 050 1

Dear Editor,

I, as corresponding author, submit the manuscript *"Degradation of wood by UV light: a study by EGA-MS and Py-GC/MS with on line irradiation system"* by Marco Mattonai, Atsushi Watanabe, Ai Shiono, and Erika Ribechini for publication in *Journal of Analytical and Applied Pyrolysis* as a full research article.

The manuscript describes the effect of UV light on the pyrolytic behaviour of wood using a recently developed instrumentation. Both a softwood and a hardwood samples were tested, and two different instrumental setups were used. First, UV irradiation followed by evolved gas analysis was used to establish the effect of irradiation on the thermal stability of the samples. Softwood was found to be significantly more affected than hardwood. Second, UV irradiation followed by analytical pyrolysis–GC/MS with *in situ* derivatisation was used o obtain a detailed screening of the composition of the pyrolysates as a function of irradiation time. The data obtained were processed with principal component analysis to outline trends in the yields of the various pyrolysis products.

We really hope that our paper could be considered for the publication in *Journal of Analytical and Applied Pyrolysis.*

I declare that the work presented in the manuscript is original and not under consideration elsewhere. All the authors approved the manuscript and agree that it should be submitted to *Journal of Analytical and Applied Pyrolysis*.

Best regards,
Marco Mattonai

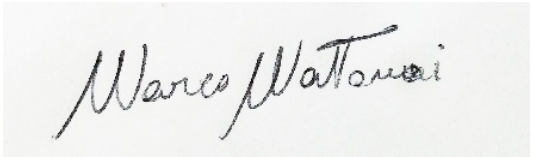

Degradation of wood by UV light: a study by EGA-MS and Py-GC/MS with on line irradiation system

Marco Mattonai[a], Atsushi Watanabe[b], Ai Shiono[b], Erika Ribechini[a]

[a] Department of Chemistry and Industrial Chemistry, University of Pisa, Via Moruzzi 13, 56124 Pisa, Italy

[b] Frontier Laboratories Ltd., 4-16-20 Saikon, Koriyama, Fukushima, 963-8862, Japan

Abstract

UV degradation of wood is an important phenomenon that entails loss of aesthetic and mechanic properties. The changes are usually studied with artificial ageing followed by spectroscopy, and focus on colour changes. Analytical pyrolysis coupled with gas chromatography-mass spectrometry (Py-GC/MS) and evolved gas analysis-mass spectrometry (EGA-MS) are powerful tools for wood characterisation, but the change in pyrolytic behaviour of wood after UV irradiation is not well documented. In this work, a new instrumental setup was used to perform UV irradiation on line with EGA-MS and Py-GC/MS with *in situ* derivatisation of fir and chestnut wood. The effect of UV exposure was evaluated in terms of thermal stability and composition of the pyrolysate. The results showed that UV degradation of wood is strongly related to its lignin content. Fir wood, with higher lignin content, showed extensive degradation after 4 hours of irradiation, while chestnut wood, with lower lignin content, showed very small changes. Holocellulose to lignin ratios (H/L) were calculated, and principal component analysis was performed on the results of Py-GC/MS, revealing that this technique could be used as a fast monitoring tool to assess the UV degradation of wood.

Keywords: Analytical pyrolysis; Evolved gas analysis; UV degradation; Biomass; Wood; Lignin

INTRODUCTION

Light exposure is a major cause for wood degradation, leading to colour change and loss in mechanical properties [1-5]. The study of changes in properties of wood after UV degradation are of paramount importance in many fields, including materials science, construction, biomass and art. Photodegradation of wood is known to be influenced by many factors, the most important ones being wood species, temperature and humidity [6-9]. UV light absorption of wood is mainly due to the aromatic structure of lignin, and leads to the formation of free radicals [10,11]. The colour change can be attributed to the oxidation of the hydroxyl groups of lignin to carbonyl groups [5,12].

Since natural weathering is not reproducible, photodegradation of lignocellulose is usually studied by artificial ageing using UV lamps, and the results of degradation are typically observed with spectroscopic techniques such as IR, UV-Vis and fluorescence [12-14]. Baur and co-workers [11] used electron paramagnetic resonance spectroscopy (EPR) to evaluate the formation of free radicals in wood after UV irradiation. The main disadvantage of these techniques is that they provide information on the whole sample, with only few structural insights on the components of lignocellulose. Moreover, as noted by Pandey and co-workers [15], the presence of additional species such as extractives in wood can lead to misinterpretation of the results.

Analytical pyrolysis coupled with GC/MS is the most widely used and flexible techniques for lignocellulose characterisation [16-22]. Py-GC/MS experiments require very small sample quantities and provide short time of analysis with good reproducibility. The chromatographic quality can also be improved using *in situ* derivatisation, which prevents tailing of compounds bearing highly polar functional groups [23-25].

Modern instrumentation for analytical pyrolysis is constantly evolving, unlocking new possibilities for detailed analyses of many types of samples. In recent years, the combination of UV-light irradiation and analytical pyrolysis was made possible and was successfully applied to study the ageing of synthetic polymers [26-29]. The results of these studies showed that UV/Py-GC/MS and UV/EGA-MS can be used as reliable techniques to gain information on the effect of UV irradiation on both the generation of volatile molecules, and the structure of the original material.

In this work, UV/EGA-MS and UV/Py-GC/MS with *in situ* derivatisation were performed on wood samples, to obtain insight on the effect of irradiation on the thermal stability and composition of lignocellulose. Both a softwood and a hardwood samples were used, and the different behaviours were compared. To the best of our knowledge, this is the first work that describes the effect of light irradiation on wood using analytical pyrolysis as a monitoring technique.

MATERIALS AND METHODS

Materials: Hexamethyldisilazane (HMDS, Sigma-Aldrich, USA) was used as a derivatising agent in all UV/Py(HMDS)-GC/MS experiments. Fir (*Abies alba*) and chestnut (*Castanea sativa*) wood were acquired as slabs from a local provider in Pisa, Italy. The slabs were cut into small pieces (approx. 5 cm length) and milled with a Pulverisette 23 ball mill (Fritsch, Germany) until a fine and homogeneous powder was obtained. Before analysis, the powder samples were also dried in oven at 50 °C for 8 hours.

Apparatus: *In situ* irradiation and pyrolysis were performed using an EGA/PY-3030D micro-furnace pyrolyser, equipped with an UV-1047Xe micro UV-irradiator and a QSP-1046E quick-stabilising pressure flow switch (Frontier Laboratories Ltd., Japan). This instrument has been described in previous publications [26,27,29]. The micro-UV irradiator is equipped with a Xe arc lamp, with emission in the range 280-450 nm. The intensity of emitted light was approximately 40 W/m^2. Irradiation took place directly inside the pyrolysis furnace at a temperature of 60 °C. To simulate natural conditions, during irradiation the pyrolysis furnace was filled with air instead of helium. When the irradiation was complete, the whole system was purged with helium for 15 min before analysis. The irradiation times were 1, 2 and 4 h. To ensure that the observed changes in pyrolytic behaviour were only caused by UV irradiation, the samples were also analysed after being kept in the pyrolysis furnace under air at 60 °C for 4 hours with no irradiation. GC/MS analyses in all experiments were performed with a 7890 gas chromatograph (Agilent Technologies, USA) coupled to a 5975 Mass Selective Detector (MSD, Agilent Technologies, USA). All analyses were carried out using helium as carrier gas (1 mL min^{-1}). The MSD was operated in EI positive mode (70 eV). The ion source was kept at 230 °C, while the quadrupole analyser was kept at 150 °C.

UV/EGA-MS setup: During UV/EGA-MS analyses, the pyrolysis furnace was heated from 60 °C to 700 °C at 10 °C min^{-1}. The pyrolysis interface was kept at 100 °C higher than the furnace temperature, up to a maximum of 300 °C. The GC inlet was at 280 °C, and operated in split mode with a 10:1 ratio. All analyses were performed using an UADTM-2.5N deactivated metal capillary tube (3 m x 0.15 mm, Frontier Laboratories Ltd., Japan), directly connecting the pyrolysis furnace to the MSD. The GC oven was kept at 60 °C during irradiation, and was raised to 300 °C during the analyses. The transfer-line was kept at 300 °C. Mass spectra were recorded in the *m/z* range 50-600. The sample amount was approximately 100 µg.

UV/Py(HMDS)-GC/MS setup: All experiments were performed with a pyrolysis temperature of 550 °C and a pyrolysis time of 0.2 min. The pyrolysis interface temperature was 280 °C. The GC inlet was at 280 °C, and operated in split mode with a 20:1 ratio. All analyses were performed with an Ultra ALLOY$^+$-1 capillary column (30m x 0.25 mm, film thickness 0.5 µm, Frontier Laboratories, Japan). During irradiation, the GC oven was kept at 40 °C to prevent column damage. During analysis, the following

temperature program was used: 50 °C isothermal for 1 min; 10 °C min^{-1} up to 100 °C, then isothermal for 2 min; 4 °C min^{-1} up to 190 °C, then isothermal for 1 min; 30 °C min^{-1} up to 280 °C, then isothermal for 20 min. The transfer-line was kept at 280 °C. Mass spectra were recorded in the *m/z* range 50-600. The sample amount was approximately 100 µg, and derivatisation was performed by adding 5 µL of HMDS immediately before the analysis.

Data processing: Both EGA-MS and Py-GC/MS data were processed with Origin Pro 8 SR0 (v8.0724, OriginLab Corporation, USA). Py-GC/MS data were also processed using the Automated Mass spectra Deconvolution and Identification Software (AMDIS, version 2.71, NIST, USA). Signals in the mass spectra of EGA thermograms were identified based on the literature [30-33]. Compounds in the pyrograms were identified based on their mass spectra, using literature references [18,23,24], Wiley and NIST-EPA-NIH reference libraries. Semi-quantitative calculations were performed by integrating the peaks of identified compounds, and then expressing the peak areas as percentages. Principal component analysis (PCA) was performed with R (version 3.10, R foundation), using percentage areas as database. Replicates of the same sample were performed to evaluate reproducibility of both UV/EGA-MS and UV/Py(HMDS)-GC/MS analyses. Relative standard deviations were 5% for EGA and 10% for Py-GC/MS on average.

RESULTS AND DISCUSSION

UV/EGA-MS: The total ion thermograms (TIT) for all samples at all irradiation times are shown in Figure 1. Each thermogram was normalised using its peak signal.

The TIT of non-irradiated fir wood showed three thermal degradation regions. The first region is between 200 and 350 °C, the second is between 350 and 400 °C, and the third is between 400 and 500 °C. After irradiation, several changes in the TIT were observed. First, there was a shift to lower temperatures of the signal peak. After 4 hours of irradiation, the shift was greater than 40 °C. The shift in the signal peak is due to a broadening of the EGA profile, which suggests that degradation of the sample was only partial. This is probably because UV light has a low penetrating power, and the internal portion of the sample remained unaffected by the irradiation. Finally, a remarkable change in the shape of the TIT was observed, and only two regions of thermal degradation could be outlined.

The average mass spectra for the non-irradiated and 4-hour irradiated samples are also shown in Figure 1. In the average mass spectrum of the non-irradiated fir sample, the characteristic peaks of softwood were observed. The signals at *m/z* 55, 57, 60, 69, 73, 85, 98, 114 and 126 are characteristic of holocellulose, while the signals at *m/z* 91, 137, 151, 164, 178 and 272 are typical of guaiacyl-lignin [30-32].

Significant changes were observed after 4 hours of irradiation. All *m/z* signals of lignin were either absent or their intensity was considerably reduced, suggesting that lignin underwent an extensive degradation after UV irradiation. This result agrees with the literature [10,11]. While the *m/z* signals of holocellulose were still present in the mass spectrum after degradation, their relative intensities were different. There was an increase in the signals at *m/z* 60 and 73, which are characteristic of levoglucosan, the main pyrolysis product of cellulose [31]. On the contrary, other holocellulose signals, such as *m/z* 85 and 114, decreased. This suggests that irradiation also caused a partial degradation of holocellulose.

The main *m/z* signals corresponding to both holocellulose and lignin were extracted from the thermograms of the non-irradiated and 4-hour irradiated samples of both wood species, to obtain information about the thermal degradation processes occurring in each thermal degradation region: *m/z* 60 and 73 for cellulose, *m/z* 85 for holocellulose, *m/z* 91 and 137 for lignin. The ion profiles are shown in Figure 2.

In the non-irradiated fir sample, the main signals of holocellulose appeared in the first and second region, while the main signals of lignin are present throughout the whole thermogram. The signals at *m/z* 60 and 73 show a peak in the second region, suggesting that cellulose pyrolysis is taking place in this portion of the thermogram. A comparison of the profiles of *m/z* 137 and *m/z* 91 also suggests that in the first region of the thermogram (peak of *m/z* 137) lignin undergoes the first thermal degradation, while in the second and third regions (peak of *m/z* 91) secondary pyrolysis takes place. These results agree with EGA-MS studies of wood [31].

After 4 hours of irradiation, the ion profiles of fir changed drastically. The signals of lignin showed very low intensities, indicating an extensive degradation. On the other hand, the signals of cellulose became dominant in the whole thermogram, while *m/z* 85 decreased. This confirms that hemicellulose was more degraded than cellulose. The broadening of the ion profiles of *m/z* 60 and 73, however, suggests that partial degradation of cellulose also took place.

The TIT profiles of chestnut samples are similar to those of fir samples, with three thermal degradation regions. However, the thermogram of chestnut is considerably narrower than the one obtained for fir. A likely explanation for this is that chestnut wood has a higher cellulose content than fir.

Contrary to fir wood, the thermograms of chestnut showed little to no variation after irradiation. A shift in the peak of signal was observed, although it was much less evident, and amounted to only 8 °C after 4 hours of irradiation. Broadening of the thermogram was also observed, but this also was less evident than the one observed for fir wood. These results suggest that UV irradiation of chestnut wood was much less effective than fir wood.

The main signals in the average mass spectra of chestnut wood were the same observed for fir wood, with some additional signals that can be attributed to syringyl-lignin: *m/z* 167, 181 and 208 [30,32,33]. In both chestnut average mass spectra, the signals of holocellulose were much higher than those of lignin. The signals at *m/z* 60 and 73, which are characteristic of cellulose, were very high even before irradiation.

In agreement with the EGA profiles, there was very little change in the average mass spectrum of chestnut after irradiation. The intensity of the lignin signals decreased slightly, but the signals of holocellulose did not show any meaningful change. The fact that the relative intensities of holocellulose signals were not affected by irradiation suggests that, despite the high abundance, the polysaccharide fraction was not significantly degraded by UV light. A possible explanation of this is that the degradation of the polysaccharide fraction is not directly induced by irradiation, but rather by the free radicals generated from UV absorption by lignin. This hypothesis has already been discussed in the literature [10,11]. It is likely that the low content of lignin, which is responsible for the absorption of UV light, does not generate enough free radicals, and therefore holocellulose remained mostly unaltered by irradiation. The case of chestnut is therefore opposite to the one of fir, in which the lignin content is sufficiently high to generate a considerable number of free radicals and cause a partial degradation of holocellulose at long irradiation times.

The ions extracted for fir wood were the same as those extracted from the EGA profiles of chestnut, with the addition of *m/z* 167 which is characteristic of syringyl-lignin. The ion profiles, which are shown in Figure 2, confirmed that cellulose is the main component of chestnut wood, and there is a low amount of lignin. The signals of holocellulose (*m/z* 60, 73 and 85) showed a peak in the first region, while the signals of lignin (*m/z* 91, 137 and 167) showed a peak in the second region. It is worth noting that the extracted ion profiles of the lignin signals in chestnut wood showed peaks at lower temperatures than in fir wood. This is because hardwood lignin has a lower C-C and a higher C-O-C bond content than softwood lignin, resulting in less thermal stability [34]. In agreement with the TIT profiles, there was very little change in the ion profiles after irradiation.

UV/Py(HMDS)-GC/MS: The pyrograms of non-irradiated and 4-hour irradiated fir and chestnut samples are shown in Figure 3, and all identified compounds are listed in Table 2. Some compounds that were not available in the literature or in reference mass spectra libraries were identified by comparison with known compounds showing similar mass spectra.

Pyrolysis of wood takes place with many competitive and parallel processes, and therefore many different products are obtained. Small molecules (#1, 3, 5, 7, 13, 25, 33, 39) and hydroxybenzenes (#21,

36, 43 ,59, 69) can be generated both by holocellulose and lignin following various pyrolysis mechanisms.

Anhydrosugars (#37, 44, 51, 52, 62, 63, 66, 70, 75, 78, 79, 82) are obtained from depolymerisation of holocellulose, which is the primary pyrolysis process. Secondary pyrolysis of holocellulose consists mainly of multiple dehydration reactions, and generates cyclopentenones (#8, 10, 16, 18, 22, 23, 27, 38, 46, 47, 49), furans (#2, 9, 29, 30, 32) and pyrans (#15, 19, 20, 26, 28, 35, 55, 65, 77). Uronic acids (#72, 84, 90, 91) are components of hemicellulose. Their presence as whole monosaccharides is likely due to a high reactivity of the carboxylic moiety towards the derivatising agent, which prevents further degradation processes. Uronic acids or their isomers could also be obtained from oxidation of monosaccharides during the irradiation of the sample.

Lignin pyrolysis starts with depolymerisation and the formation of whole monomers (#86, 87, 92, 95, 98, 99). Secondary pyrolysis of lignin mainly involves the cleavage of the alkyl chain or the loss of the aliphatic hydroxyl group, leading to the formation of shortened chain compounds (#6, 17, 24, 31, 34, 40, 41, 45, 48, 50, 54, 60, 64, 68, 76, 88, 94). Loss of methyl or methoxyl groups from the aromatic ring can also take place, generating demethylated products (#42, 53, 58, 83, 97, 100). If both the cleavage of the alkyl chain and the demethylation take place, simple phenolic compounds are obtained (#4, 11, 12, 14). Some oxidised monomers, and fragments thereof, were also found in the pyrograms (#56, 57, 61, 67, 71, 73, 74, 80, 81, 85, 89, 93). The presence of these compounds could be due to both rearrangements reactions during lignin depolymerisation, and to oxidation reactions that took place during the irradiation.

The pyrograms of non-irradiated and 4 hours irradiated fir and chestnut samples are shown in Figure 3. The pyrogram of non-irradiated fir was dominated by the two peaks of guaiacyl alcohol isomers (#86, 87, 92). Other intense peaks were observed for some furans and pyrans (#32, 46 and 65). Small molecules generated very low peaks.

After irradiation, the complexity of the pyrogram increased. The peak height of the two lignin monomers decreased considerably, while the height of many of the other peaks increased. The most evident increase was observed for some small molecules (#5, 7 and 25) and some anhydrosugars (#63, 70, 78). The increase in small molecules after irradiation is an indication of a lower thermal stability of fir wood, which is consistent with the EGA results. The increase in the yield of anhydrosugars suggests that depolymerisation is the most likely degradation process of holocellulose in this case. In fact, it has been shown that the yield of anhydrosugars increases with the decrease of polymerisation degree during the pyrolysis of carbohydrates in the presence of hexamethyldisilazane [24].

The pyrogram of non-irradiated chestnut was considerably different from that of fir. The increased number of peaks is due to the more complex structure of hardwood lignin, in which both guaiacyl

alcohols (#86, 87, 92) and synapyl alcohols (#95, 98 and 99) are present. The yield of anhydrosugars in chestnut wood is very high, which is consistent with the EGA results suggesting a high holocellulose content. It is interesting to notice that mono-derivatised anhydrosugars (#51 and 52) showed very high peaks compared to non-irradiated fir, meaning that derivatisation of holocellulose is less efficient for chestnut. This could be due to different arrangements of holocellulose and lignin in the two wood species.

Another interesting feature of the pyrograms of chestnut is the presence of gallic acid (#96). This compound is a well-known antioxidant, and could be partially responsible for the resistance of chestnut to UV degradation (alone or with other polyphenols that were not detected by this analysis). The role of tannins in increasing the resistance to photo-degradation of wood has already been observed in the literature [15,35].

As expected from the EGA results, there was very little change in the pyrogram of chestnut even after 4 hours of irradiation. As observed for fir wood, there was a significant decrease in the peaks of lignin monomers, confirming the UV degradation of lignin. The peak of gallic acid also decreased, suggesting that it could have acted as radical scavenger and reduced UV degradation. Moreover, the peak height ratio between mono-derivatised anhydrosugars (#51, 52) and bi- and tri-derivatised anhydrosugars (#62, 63, 66, 70, 75, 78, 79, 82) decreased considerably after irradiation. This means that derivatisation was more efficient for the irradiated chestnut sample than for the non-irradiated one. This could be due to an alteration of the spatial arrangement of the polysaccharide chains after UV exposure. For instance, the degradation of the lignin fraction could have caused an increase in the disorder of the cellulose strands, with a reduction of the crystallinity index. Since the crystalline structure of cellulose is due to the hydrogen bonds between hydroxyl groups, an amorphization process could have increased the reactivity of these groups towards derivatisation.

To evaluate the changes in composition of the pyrolysate, the holocellulose-to-lignin (H/L) ratios were calculated for all samples by dividing the total area of holocellulose pyrolysis products by the total area of lignin pyrolysis products. The results are summarised in Table 1. Starting H/L values were 1.2 for fir wood and 5.6 for chestnut wood. After irradiation, an increase in H/L was observed for both samples, consistently with the degradation of lignin. However, different trends were observed for the two wood species. After 2 hours, the H/L increased by 25% (from 5.6 to 7.1) for chestnut, and by over 300% (from 1.2 to 5.3) for fir. After 4 hours of irradiation, the two species showed different trends: the H/L value of chestnut increased again, while the value for fir decreased. This is most likely due to a partial degradation of holocellulose in fir at long irradiation times.

To evaluate the change in pyrolytic behaviour of the samples after irradiation, percentage yields were calculated for all pyrolysis product categories. Calculations were performed by imposing the total area

for both holocellulose and lignin-exclusive pyrolysis products equal to 100. The yield of small molecules and hydroxybenzenes, which were not considered as exclusive of holocellulose or lignin, were calculated by dividing their total area for the area of all peaks. In this way, the observed yield changes were independent from the total change in composition of the pyrolysate. The results are summarised in Table 1.

The two wood species showed similar trends. When irradiation time was increased, the yield of small molecules increased considerably for fir wood, and to a lesser extent for chestnut wood. This is consistent with the lower thermal stability of samples after irradiation. The yield of hydroxybenzenes did not show any meaningful trend. Regarding the pyrolysis products of holocellulose, irradiation caused an increase in the yield of anhydrosugars at the expense of furans and pyrans. As already mentioned, this increase could be due to depolymerisation of the polysaccharide chains. The yield of uronic acids increased as well for fir wood, indicating that UV light caused partial oxidation of holocellulose in this species. The yield of uronic acids for chestnut increased only slightly within the first hour of irradiation, and remained constant at longer irradiation times.

Regarding the pyrolysis products of lignin, irradiation caused an increase in the phenols and oxidised compounds, at the expense of short chain products and whole lignin monomers. This result suggests that the effect of UV on lignin is the cleavage and oxidation of the alkyl side chain of guaiacyl and syringyl units, generating carbonyl and carboxyl groups.

To highlight the differences in the pyrolytic behaviour of the samples, principal component analysis (PCA) was performed using the percentage category yields as database. The loading and score plots for the first two principal components, which accounted for more than 88% of the total variance, are shown in Figure 4. The first principal component showed main contributions from most of the pyrolysis products of both holocellulose and lignin. This first component is most likely highlighting the differences between fir and chestnut. The second principal component showed contributions from all the pyrolysis products whose yield increased when irradiation time was increased: small molecules, oxidised compounds, phenols and uronic acids. This component can therefore be related to the photo-degradation and oxidation of wood after irradiation. This is also confirmed by the fact that the sample loadings shift to higher values of the second principal component as irradiation time is increased.

CONCLUSIONS

A new pyrolysis system equipped with on line UV irradiation was used to study the degradation of fir and chestnut after exposure to UV light, using two different instrumental setups.

The UV/EGA-MS setup allowed us to estimate the effect of UV light on the thermal stability of wood and its components. Fir wood showed extensive degradation, affecting mainly lignin and, to a lesser

extent, holocellulose. The shape of the thermogram of fir wood was deeply altered by UV irradiation, showing broadening and peak shift. On the other hand, chestnut wood showed little to no change in the thermograms, most likely due to the lower lignin content.

The UV/Py-GC/MS with *in situ* silylation setup was used to evaluate the changes in composition and the pyrolytic behaviour of the two wood species after UV irradiation. In agreement with the results of UV/EGA-MS analyses, fir wood showed significant changes after UV exposure, including an increase in the H/L ratio, and higher yields of both small molecules and anhydrosugars. Similar changes were observed for chestnut wood, although to a much lesser extent.

Principal component analysis performed on percentage category yields could distinguish softwood and hardwood along the first principal component, and the photo-degradation of the samples along the second principal component.

The results of this work prove that analytical pyrolysis with *in situ* derivatisation can be used as a screening method to assess the degradation of wood by UV light, providing the advantage of short times, low sample amounts and high reproducibility. Moreover, the changes in the pyrolytic behaviour due to UV light exposure could be exploited in the field of biomass pyrolysis, to favour the formation of specific compounds and obtain pyrolysis mixtures with more desirable characteristics.

REFERENCES

[1] L. Tolvaj and K. Mitsui, *Journal of Wood Science*, 51, (2005) 468.

[2] D.N.S. Hon and S.T. Chang, *Journal of Polymer Science: Polymer Chemistry Edition*, 22, (1984) 2227.

[3] R. Garcia, M.C. Triboulot, A. Merlin and X. Deglise, *Wood Science and Technology*, 34, (2000) 99.

[4] B. George, E. Suttie, A. Merlin and X. Deglise, *Polymer Degradation and Stability*, 88, (2005) 268.

[5] D.N.-S. Hon and N. Shiraishi, *Wood and cellulosic chemistry, revised, and expanded*, CRC Press, 2000, p.

[6] X. Colom, F. Carrillo, F. Nogués and P. Garriga, *Polymer Degradation and Stability*, 80, (2003) 543.

[7] L. Tolvaj, Z. Molnar and R. Nemeth, *Journal of Photochemistry and Photobiology B: Biology*, 121, (2013) 32.

[8] E. Preklet, L. Tolvaj, L. Bejo and D. Varga, *Journal of Photochemistry and Photobiology A: Chemistry*, 356, (2018) 329.

[9] D.N.-S. Hon, *Wood and fiber science*, 26, (2007) 185.

[10] C.-M. Popescu, M.-C. Popescu and C. Vasile, *International Journal of Biological Macromolecules*, 48, (2011) 667.

[11] S.I. Baur and A.J. Easteal, *Holzforschung*, 68, (2014) 775.

[12] K.K. Pandey, *Polymer Degradation and Stability*, 90, (2005) 9.

[13] K.K. Pandey and T. Vuorinen, *Polymer Degradation and Stability*, 93, (2008) 2138.

[14] U. Müller, M. Rätzsch, M. Schwanninger, M. Steiner and H. Zöbl, *Journal of Photochemistry and Photobiology B: Biology*, 69, (2003) 97.

[15] K.K. Pandey, *Polymer Degradation and Stability*, 87, (2005) 375.

[16] C. Mukarakate, A. Mittal, P.N. Ciesielski, S. Budhi, L. Thompson, K. Iisa, M.R. Nimlos and B.S. Donohoe, *ACS Sustainable Chemistry & Engineering*, 4, (2016) 4662.

[17] M. Mattonai, D. Licursi, C. Antonetti, A.M. Raspolli Galletti and E. Ribechini, *Journal of Analytical and Applied Pyrolysis*, (2017).

[18] D. Tamburini, J.J. Łucejko, M. Zborowska, F. Modugno, W. Prądzyński and M.P. Colombini, *Journal of Analytical and Applied Pyrolysis*, 115, (2015) 7.

[19] T. Ohra-aho, F.J.B. Gomes, J.L. Colodette and T. Tamminen, *Journal of Analytical and Applied Pyrolysis*, 101, (2013) 166.

[20] S. Wang, K. Wang, Q. Liu, Y. Gu, Z. Luo, K. Cen and T. Fransson, *Biotechnology Advances*, 27, (2009) 562.

[21] A.M. Azeez, D. Meier, J. Odermatt and T. Willner, *Energy & Fuels*, 24, (2010) 2078.

[22] S.C. Moldoveanu, *Analytical Pyrolysis of Natural Organic Polymers*, Elsevier Science, Amsterdam, 1998, p.

[23] D. Fabbri and G. Chiavari, *Analytica Chimica Acta*, 449, (2001) 271.

[24] M. Mattonai, D. Tamburini, M.P. Colombini and E. Ribechini, *Analytical Chemistry*, 88, (2016) 9318.

[25] C. Torri, E. Soragni, S. Prati and D. Fabbri, *Microchemical Journal*, 110, (2013) 719.

[26] T. Yuzawa, C. Watanabe, S. Tsuge, N. Shimane and H. Imai, *Polymer Degradation and Stability*, 96, (2011) 91.

[27] C. Watanabe, S. Tsuge and H. Ohtani, *Polymer Degradation and Stability*, 94, (2009) 1467.

[28] K. Matsui, A. Hosaka, A. Watanabe, N. Teramae and H. Ohtani, *Polymer Testing*, 56, (2016) 54.

[29] T. Yuzawa, C. Watanabe, N. Nemoto and H. Ohtani, *Polymer degradation and stability*, 98, (2013) 671.

[30] A.D. Pouwels, G.B. Eijkel and J.J. Boon, *Journal of Analytical and Applied Pyrolysis*, 14, (1989) 237.

[31] D. Tamburini, J.J. Łucejko, E. Ribechini and M.P. Colombini, *Journal of Mass Spectrometry*, 50, (2015) 1103.
[32] G.C. Galletti and P. Bocchini, *Rapid Communications in Mass Spectrometry*, 9, (1995) 815.
[33] J.J. Łucejko, F. Modugno, E. Ribechini and J.C. del Río, *Analytica Chimica Acta*, 654, (2009) 26.
[34] S. Wang, G. Dai, H. Yang and Z. Luo, *Progress in Energy and Combustion Science*, 62, (2017) 33.
[35] E. Tomak and O. Gonultas, *Journal of Wood Chemistry and Technology*, 38, (2018) 183.

Table 1: Temperature values for the degradation range, temperature of signal peaks from UV/EGA-MS analyses, H/L and percentage category yields for all samples. The degradation ranges were determined using the temperatures at which the signal intensity reaches 5% of the maximum intensity. Smo = small molecules, Hyb = hydroxybenzenes, Cyp = cyclopentenones, Fur = furans, Pyr = pyrans, Ahs = anhydrosugars, Ura = uronic acids, Phe = phenols, Cha = shortened chain, Dem = demethylated, Oxd = oxidised, Mon = lignin monomers.

	Fir wood				**Chestnut wood**			
Irrad. time (h)	0	1	2	4	0	1	2	4
Deg. range (°C)	243-453 (210)	216-464 (248)	203-474 (271)	193-469 (276)	235-397 (162)	225-409 (184)	222-400 (178)	223-409 (186)
EGA peak (°C)	370	359	337	326	296	293	286	288
H/L	1.2	3.2	5.3	4.7	5.6	6.4	7.1	9.1
Smo	6.6	10.4	11.8	12.0	3.1	4.3	5.5	5.6
Hyb	4.7	6.2	4.9	5.6	3.4	3.0	3.8	2.7
Cyp	41.5	27.4	22.3	21.0	16.8	14.8	14.5	13.4
Fur	13.5	5.5	4.8	5.3	3.3	3.8	3.6	3.1
Pyr	34.9	27.2	23.5	24.8	21.4	22.1	21.2	18.1
Ahs	10.0	38.2	46.8	46.1	58.4	58.7	60.3	64.9
Ura	0.0	1.6	2.5	2.7	0.1	0.5	0.4	0.4
Phe	0.8	2.3	3.3	2.7	0.6	0.8	1.7	1.4
Cha	30.0	30.5	29.3	29.6	55.2	51.8	48.8	45.3
Dem	1.3	3.1	3.6	2.6	4.5	1.7	2.7	1.9
Oxd	12.4	20.1	23.6	23.5	7.3	15.1	18.8	20.4
Mon	55.6	44.0	40.2	41.6	32.4	30.6	28.0	31.1

Table 2: Identified compounds from the UV/Py(HMDS)-GC/MS analyses of chestnut and fir wood. For each compound, the original wood component (Orig.), category (Cat.) and main *m/z* signals are shown. H = holocellulose, L = lignin; Smo = small molecules, Hyb = hydroxybenzenes, Fur = furans, Pyr = pyrans, Ahs = anhydrosugars, Cyp = cyclopentenones, Cha = shortened chain, Dem = demethylated, Phe = phenols, Mon = monomers, Oxd = oxidised. Compounds labelled with [F] or [C] were found only in the pyrograms of fir or chestnut wood, respectively.

#	Compound	Orig.	Cat.	*m/z*
1	1,2-dihydroxyethene (2TMS)	-	Smo	73, 189, 204
2	2-hydroxymethylfuran (TMS)	H	Fur	73, 81, 111, 125, 142, 155, 170
3	1,2-dihydroxyethane (2TMS)	-	Smo	73, 103, 147, 191
4	phenol (TMS)	L	Phe	75, 151, 166
5	2-hydroxypropanoic acid (2TMS)	-	Smo	73, 117, 147, 190
6	guaiacol	L	Cha	81, 109, 124
7	2-hydroxyacetic acid (2TMS)	-	Smo	73, 147, 177, 205
8	1-hydroxy-1-cyclopenten-3-one (TMS)	H	Cyp	73, 81, 101, 111, 127, 155, 169
9	2-furancarboxylic acid (TMS)	H	Fur	73, 95, 125, 169, 184
10	2-hydroxy-1-cyclopenten-3-one (TMS)	H	Cyp	73, 81, 101, 111, 127, 155, 170
11	*o*-cresol (TMS)	L	Phe	73, 91, 135, 149, 165, 180
12	*m*-cresol (TMS)	L	Phe	73, 91, 165, 180
13	3-hydroxypropanoic acid (2TMS)	-	Smo	73, 75, 147, 177, 219
14	*p*-cresol (TMS)	L	Phe	73, 91, 165, 180
15	3-hydroxy-(2H)-pyran-2-one (TMS)	H	Pyr	75, 95, 125, 151, 169, 184
16	3-hydroxycyclopenta-1,2-dione (TMS)	H	Cyp	73, 115, 143, 171, 186
17	4-methylguaiacol	L	Cha	95, 123, 138
18	2-hydroxycyclopenta-2,3-dione (TMS)	H	Cyp	73, 75, 101, 143, 171
19	5-hydroxy-2H-pyran-4(3H)-one (TMS)	H	Pyr	73, 75, 101, 129, 143, 171, 186
20	3-hydroxy-(4H)-pyran-4-one (TMS)	H	Pyr	95, 169
21	1,2-dihydroxybenzene (TMS)	H	Hyb	75, 91, 136, 151, 166, 167, 182
22	1-hydroxy-2-methylcyclopent-1-en-3-one (TMS)	H	Cyp	139, 169
23	1-methy-2-hydroxycyclopent-1-en-3-one (TMS)	H	Cyp	73, 169, 184
24	guaiacol (TMS)	L	Cha	136, 151, 166, 181, 196
25	dihydroxyacetone (2TMS)	H	Smo	73, 103, 147, 189, 219
26	2-methyl-3-hydroxy-(4H)-pyran-4-one (TMS)	H	Pyr	153, 183
27	2-methyl-3-hydroxymethyl-2-cyclopentenone (TMS)	H	Cyp	183, 198
28	3-hydroxy-6-methyl-(2H)-pyran-2-one (TMS) [C]	H	Pyr	75, 168, 183, 198
29	2-furyl-hydroxymethylketone (TMS)	H	Fur	73, 95, 103, 125, 183
30	2,3-dihydrofuran-2,3-diol (2TMS)	H	Fur	73, 133, 147, 157, 2321, 246
31	4-vinylguaiacol	L	Cha	107, 135, 150
32	5-hydroxymethyl-2-furaldehyde (TMS)	H	Fur	73, 81, 109, 111, 139, 169, 183
33	glycerol (3TMS)	H	Smo	73, 103, 117, 133, 147, 205, 218
34	4-methylguaiacol (TMS)	L	Cha	180, 195, 210
35	2-hydroxymethyl-2,3-dihydropyran-4-one (TMS)	H	Pyr	170, 185, 200
36	1,2-dihydroxybenzene (2TMS)	H	Hyb	73, 136, 151, 166, 239, 254

37	1,4:3,6-dianhydro-a-D-glucopyranose (TMS)	H	Ahs	73, 81, 103, 129, 145, 155, 170
38	1-hydroxycyclopenta-2,3-dione, enolic form (2TMS)	H	Cyp	73, 147, 169, 230, 243, 258
39	2,3-dihydroxypropanoic acid (3TMS)	-	Smo	73, 103, 117, 133, 147, 189, 205
40	syringol (TMS) [C]	L	Cha	153, 181, 196, 211, 226
41	4-ethylguaiacol (TMS)	L	Cha	179, 194, 209, 224
42	4-methylcatechol (2TMS)	L	Dem	73, 180, 253, 268
43	1,4-dihydroxybenzene (2TMS)	H	Hyb	239, 254
44	arabinofuranose (4TMS)	H	Ahs	73, 143, 147, 217, 230
45	4-vinylguaiacol (TMS)	L	Cha	162, 177, 192, 207, 222
46	2-hydroxycyclopenta-1,3-dione, enolic form (2TMS)	H	Cyp	73, 243, 258
47	3-hydroxy-2-hydroxymethyl-2-cyclopentenone (2TMS)	H	Cyp	257, 272
48	eugenol (TMS)	L	Cha	179, 206, 221, 236
49	3-hydroxy-2-(hydroxymethyl)cyclopenta-2,4-dienone (2TMS)	H	Cyp	73, 255. 270
50	4-methylsyringol (TMS) [C]	L	Cha	167, 195, 210, 225, 40
51	1,6-anydro-beta-D-glucopyranose (TMS at position 4)	H	Ahs	73, 75, 129, 145, 155
52	1,6-anydro-beta-D-glucopyranose (TMS at position 2)	H	Ahs	73, 75, 101, 116, 132, 145, 155
53	3-(methoxy)benzene-1,2-diol (2TMS)	L	Dem	153, 239, 254, 269, 284
54	Z-isoeugenol (TMS) [F]	L	Cha	73, 206, 221, 236
55	3,5-dihydroxy-2-methyl-(4H)-pyran-4-one (2TMS)	H	Pyr	73, 147, 271
56	vanillin (TMS)	L	Oxd	194, 209, 224, 239
57	2-(methoxy)benzene-1,4-diol (2 TMS)	L	Oxd	254, 269, 284
58	5-methyl-3-(methoxy)benzene-1,2-diol (2TMS) [C]	L	Dem	73, 210, 253, 268, 283, 298
59	1,2,3-trihydroxybenzene (3TMS)	H	Hyb	73, 133, 239, 327, 342
60	Z-isoeugenol (TMS)	L	Cha	206, 221, 236
61	4-hydroxybenzoic acid (2TMS)	L	Oxd	73, 193, 223, 267, 282
62	1,6-anydro-D-galactopyranose (2TMS)	H	Ahs	73, 142, 145, 161, 189, 204
63	1,4-anydro-D-galactopyranose (2TMS)	H	Ahs	73, 101, 116, 129, 145, 155, 217
64	4-vinylsyringol (TMS) [C]	L	Cha	179, 222, 237, 252
65	2-hydroxymethyl-5-hydroxy-2,3-dihydro-(4H)-pyran-4-one (2TMS)	H	Pyr	73, 129, 147, 155, 183, 273, 288
66	1,4-anydro-D-glucopyranose (2TMS) [C]	H	Ahs	73, 101, 116, 129, 155
67	acetovanillone (TMS)	L	Oxd	193, 208, 223, 238
68	Z-propenylsyringol (TMS) [C]	L	Cha	205, 221, 236, 251, 266
69	1,2,4-trihydroxybenzene (3TMS)	H	Hyb	73, 239, 327, 342
70	1,6-anydro-beta-D-glucopyranose (2TMS)	H	Ahs	73, 75, 116, 129, 191, 204, 217
71	vanillic acid methyl ester (TMS) [F]	L	Oxd	73, 193, 224, 239, 254
72	arabinonic acid-gamma lactone (3TMS)	H	Ura	73, 117, 147, 189, 204, 217, 244
73	4-hydroxy-3,5-(dimethoxy)cinnamic acid methyl ester (TMS) [C]	L	Oxd	280, 295, 310
74	syringaldehyde (TMS) [C]	L	Oxd	224, 239, 254
75	1,4-anydro-D-galactopyranose (3TMS)	H	Ahs	73, 147, 157, 191, 217, 243
76	E-propenylsyringol (TMS) [C]	L	Cha	205, 236, 251, 266
77	2,3,5-trihydroxy-4H-pyran-4-one (3TMS)	H	Pyr	73, 147, 255, 330, 345, 360
78	1,6-anydro-beta-D-glucopyranose (3TMS)	H	Ahs	73, 129, 147, 204, 217, 333
79	1,4-anhydro-D-glucopyranose (3TMS)	H	Ahs	73, 147, 157, 191, 217, 332
80	acetosyringone (TMS) [C]	L	Oxd	223, 238, 253, 268

81	vanillic acid (2TMS)	L	Oxd	126, 226, 253, 267, 282, 297, 312
82	1,6-anydro-beta-D-glucofuranose (3TMS)	H	Ahs	73, 101, 116, 129, 191, 217
83	p-coumaryl alcohol (2 TMS)	L	Dem	236, 294, 309, 324, 331
84	3-deoxy-D-arabino hexonic acid gamma lactone [F]	H	Ura	73, 103, 129, 127, 145, 205, 246
85	coniferylaldehyde (TMS) [F]	L	Oxd	73, 177, 192, 220, 235, 250
86	Z-coniferyl alcohol (TMS)	L	Mon	73, 91, 103, 131, 162, 204, 252
87	Z-coniferyl alcohol (2TMS)	L	Mon	73, 91, 103, 131, 162, 204, 252
88	3-vanillylpropanol (2TMS)	L	Cha	179, 206, 221, 236, 311, 326
89	syringic acid (2TMS) [C]	L	Oxd	223, 253, 283, 297, 312, 327, 342
90	gluconic acid lactone (4TMS) [F]	H	Ura	73, 103, 129, 147, 220, 319, 333
91	altronic acid lactone (4TMS)	H	Ura	73, 147, 189, 204, 217
92	E-coniferyl alcohol (2 TMS)	L	Mon	73, 204, 219, 235, 293, 309, 324
93	3,4-dihydroxy-5-methoxy benzoic acid (3TMS) [C]	L	Oxd	73, 223, 385, 400
94	3-syringylpropanol (2TMS) [C]	L	Cha	210, 225, 236, 240, 326, 341, 356
95	Z-synapyl alcohol (2TMS) [C]	L	Mon	73, 204, 234, 323, 339, 354
96	gallic acid (4TMS) [C]	-	-	73, 147, 179, 281, 443, 458
97	3,4-dihydroxy cinnamyl alcohol (3TMS)	L	Dem	179, 205, 293, 355, 382
98	E-synapyl alcohol (TMS) [C]	L	Mon	73, 234, 251, 267, 282
99	E-synapyl alcohol (2TMS) [C]	L	Mon	73, 234, 265, 293, 323, 339, 354
100	E-2-methoxy-3,4-dihydroxy cinnamic alcohol (3TMS)	L	Dem	73, 204, 235, 323, 381, 397, 412

386

387

Figure 1: Top – normalised total ion thermograms for all samples of fir (left) and chestnut (right). Centre – average mass spectra for non-irradiated fir (left) and chestnut (right). Bottom – average mass spectra for 4-hour irradiated fir (left) and chestnut (right).

Figure 2: Extracted ion profiles from the non-irradiated and 4-hour irradiated sample thermograms of fir (top) and chestnut (bottom).

Figure 3: Pyrograms for non-irradiated and 4-hour irradiated fir and chestnut wood samples. Peaks are numbered according to Table 1.

Figure 4: Loading plot and score plot for the PCA of all wood samples using percentage category yields as database. The samples in the score plot are labelled with the wood species and number of hours of irradiation. The arrows highlight the shift in the scores of the samples after UV irradiation.

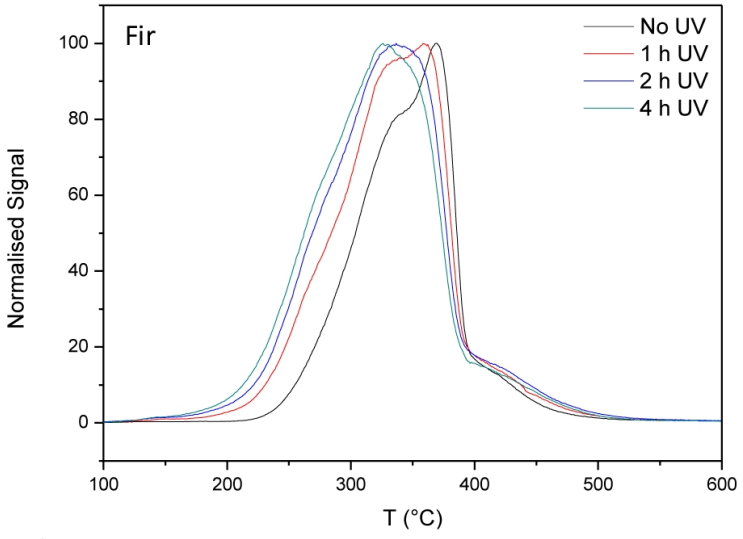
Fir
No UV
1 h UV
2 h UV
4 h UV
Normalised Signal
T (°C)

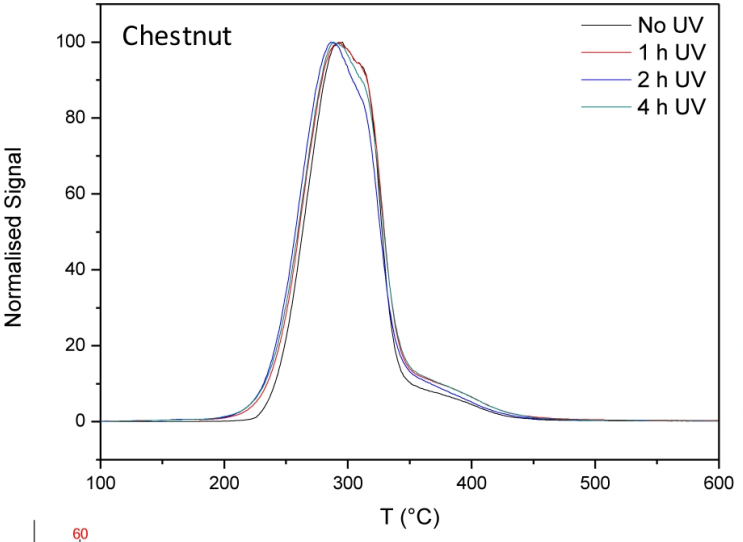
Chestnut
No UV
1 h UV
2 h UV
4 h UV
Normalised Signal
T (°C)

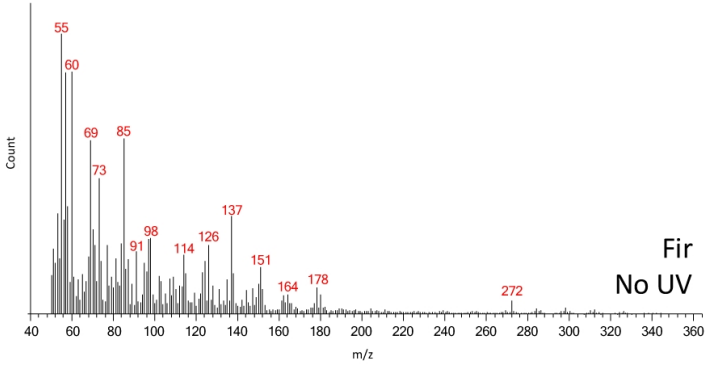
Fir
No UV
Count
m/z

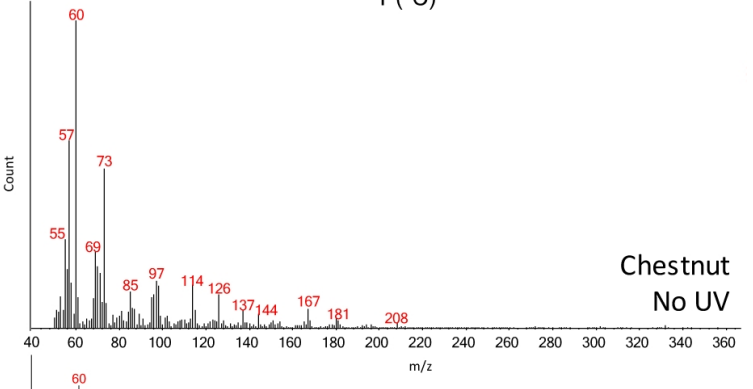
Chestnut
No UV
Count
m/z

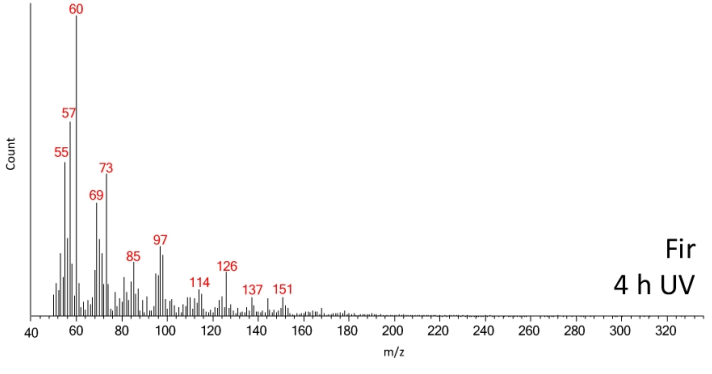
Fir
4 h UV
Count
m/z

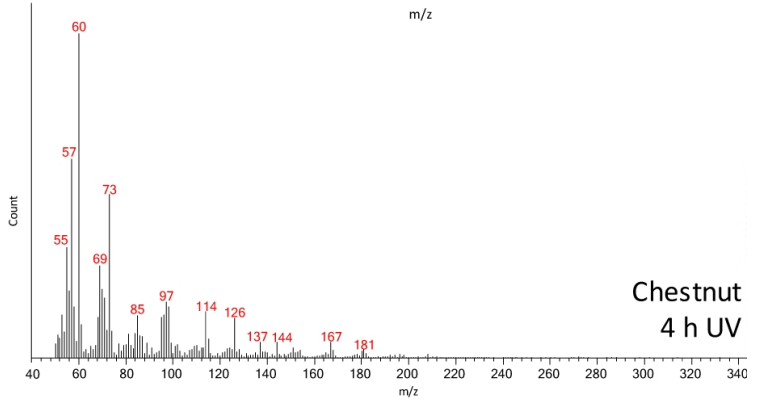
Chestnut
4 h UV
Count
m/z

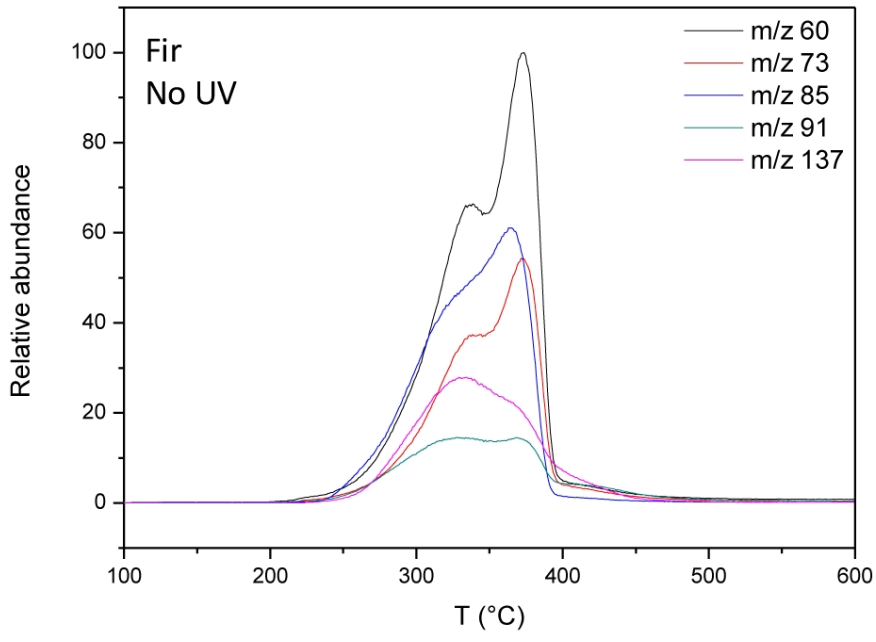
Fir
No UV
m/z 60
m/z 73
m/z 85
m/z 91
m/z 137
Relative abundance
T (°C)

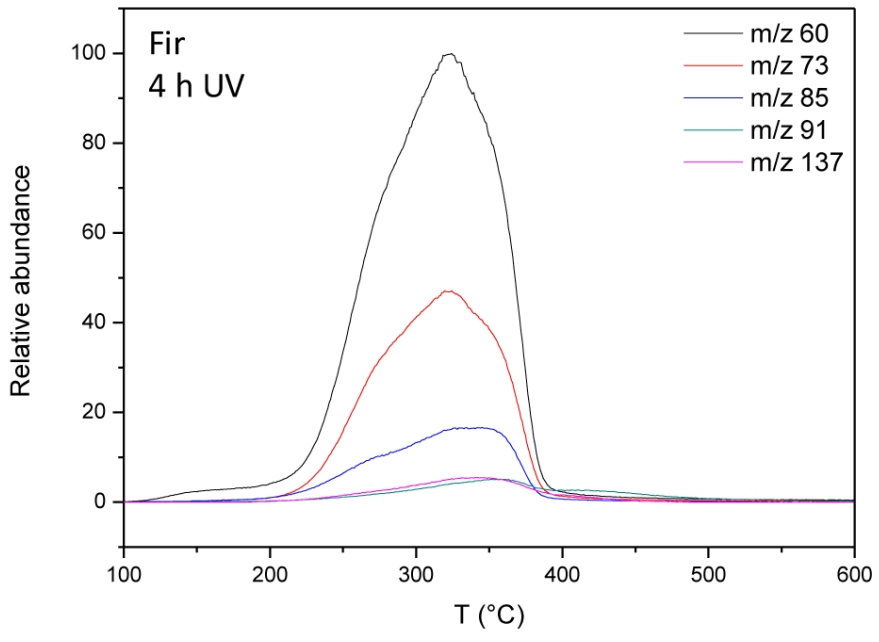
Fir
4 h UV
m/z 60
m/z 73
m/z 85
m/z 91
m/z 137
Relative abundance
T (°C)

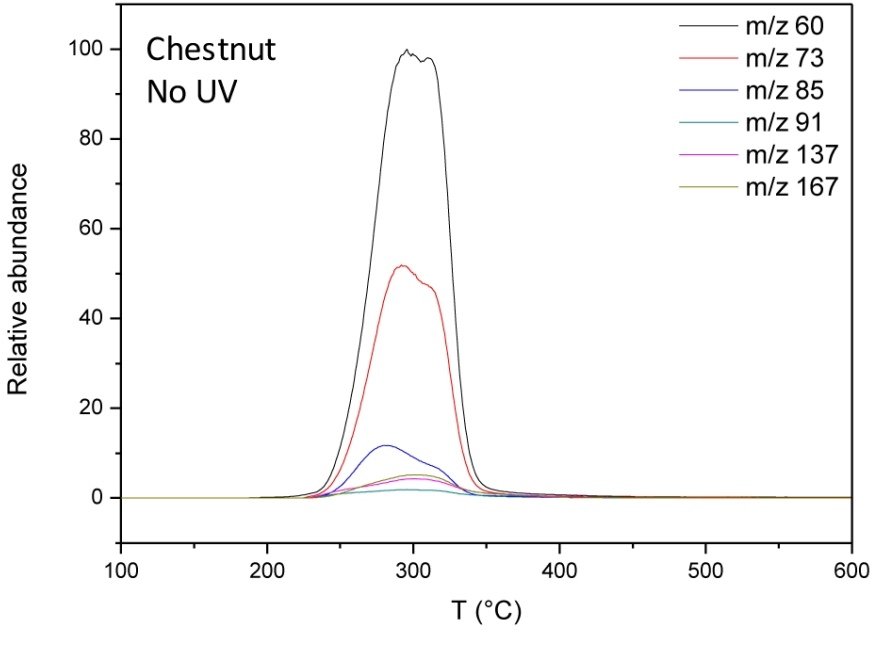
Chestnut
No UV
m/z 60
m/z 73
m/z 85
m/z 91
m/z 137
m/z 167
Relative abundance
T (°C)

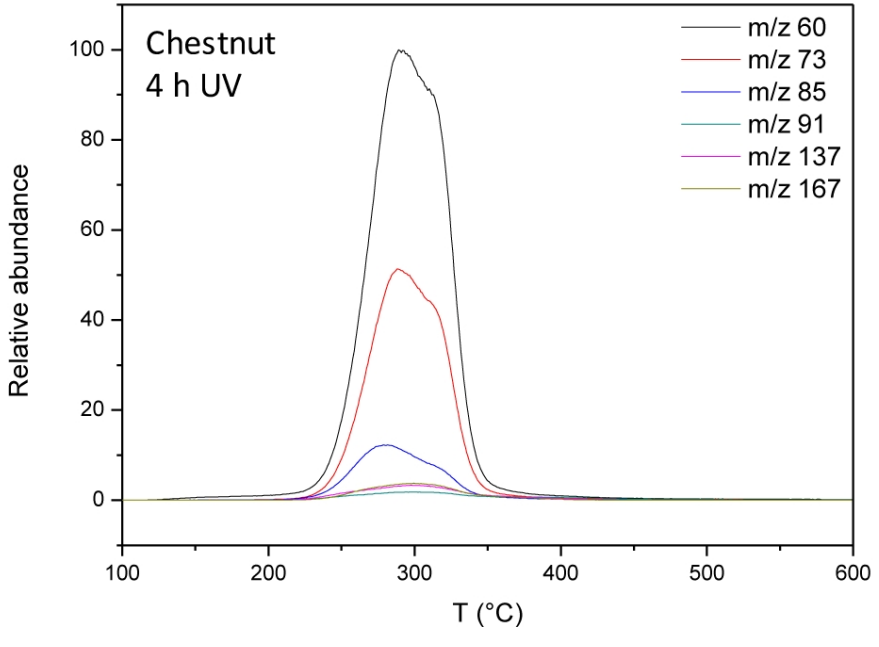
Chestnut
4 h UV
m/z 60
m/z 73
m/z 85
m/z 91
m/z 137
m/z 167
Relative abundance
T (°C)

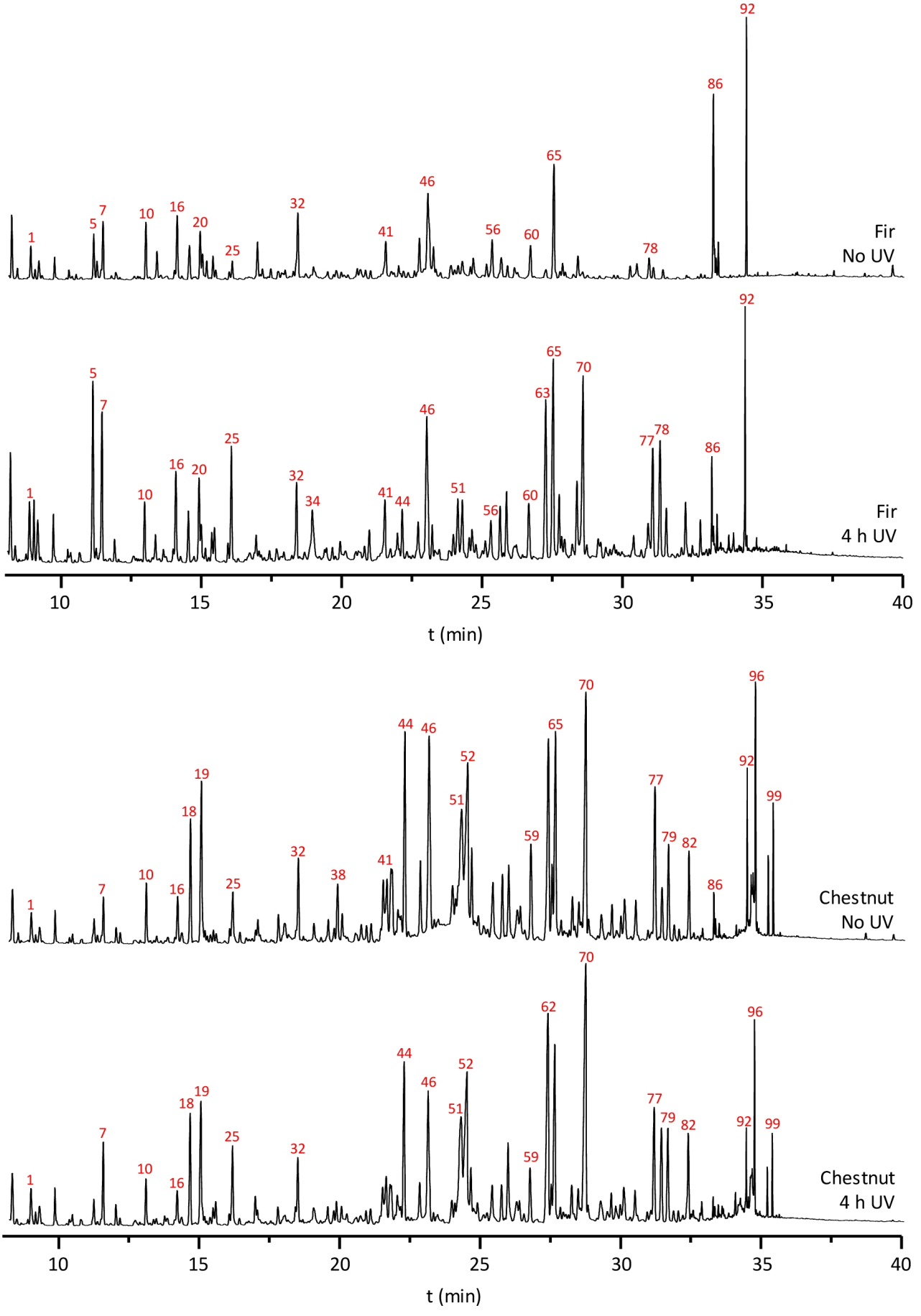
Fir
No UV
Fir
4 h UV
Chestnut
No UV
Chestnut
4 h UV
t (min)
t (min)

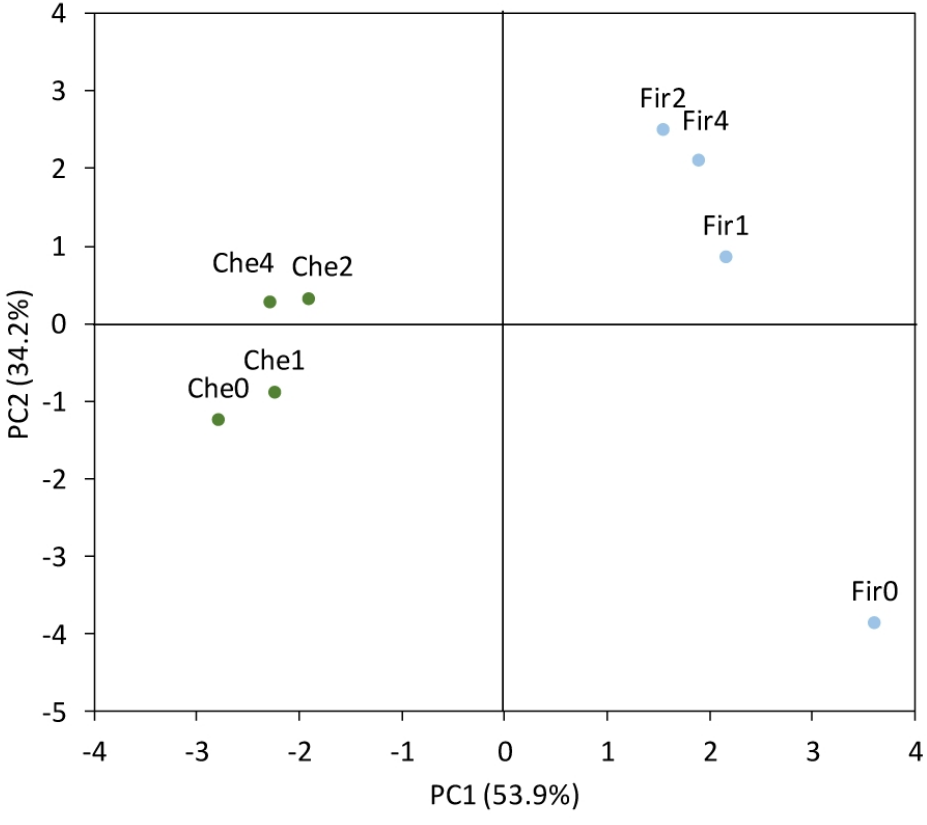
Fir2
Fir4
Fir1
Che4
Che2
Che1
Che0
Fir0
PC2 (34.2%)
PC1 (53.9%)

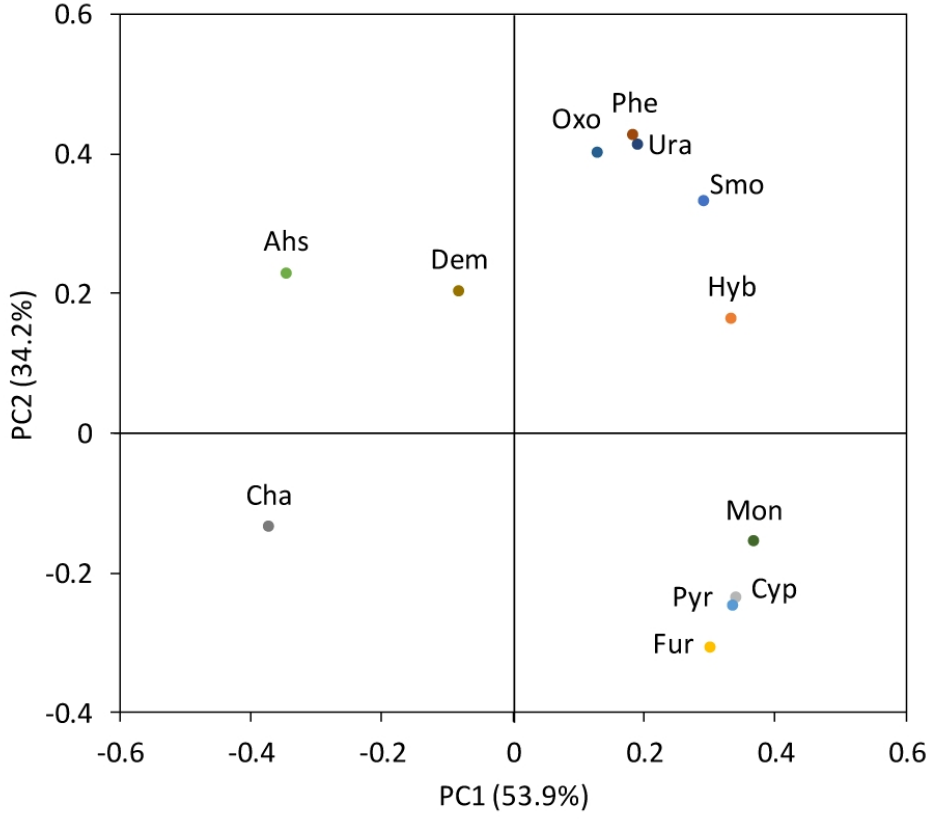
Oxo
Phe
Ura
Smo
Ahs
Dem
Hyb
Cha
Mon
Pyr
Cyp
Fur
PC2 (34.2%)
PC1 (53.9%)